

## RESEARCH ARTICLE

# Interplay in neural functions of cell adhesion molecule close homolog of L1 (CHL1) and Programmed Cell Death 6 (PDCD6)

Gabriele Loers<sup>1</sup> | Thomas Theis<sup>2</sup>  | Helen Baixia Hao<sup>2</sup> | Ralf Kleene<sup>1</sup>  |  
Sanjana Arsha<sup>2</sup> | Nina Samuel<sup>2</sup> | Neha Arsha<sup>2</sup> | Wise Young<sup>2</sup> | Melitta Schachner<sup>2</sup>

<sup>1</sup>Zentrum für Molekulare Neurobiologie, Universitätsklinikum Hamburg-Eppendorf, Hamburg, Germany

<sup>2</sup>Keck Center for Collaborative Neuroscience and Department of Cell Biology and Neuroscience, Rutgers University, Piscataway, NJ, USA

## Correspondence

Melitta Schachner, Keck Center for Collaborative Neuroscience and Department of Cell Biology and Neuroscience, Rutgers University, 604 Allison Road, Piscataway, NJ 08854, USA.  
Email: schachner@dls.rutgers.edu

## Funding information

Support by the Keck Center of Rutgers University.

## Abstract

Close homolog of L1 (CHL1) is a cell adhesion molecule of the immunoglobulin superfamily. It promotes neurite outgrowth and survival of neurons in vitro. In vivo, CHL1 promotes nervous system development, regeneration after trauma, and synaptic function and plasticity. We identified programmed cell death 6 (PDCD6) as a novel binding partner of the CHL1 intracellular domain (CHL1-ICD). Co-immunoprecipitation, pull-down assay with CHL1-ICD, and proximity ligation in cerebellum and pons of 3-day-old and 6-month-old mice, as well as in cultured cerebellar granule neurons and cortical astrocytes indicate an association between PDCD6 and CHL1. The Ca<sup>2+</sup>-chelator BAPTA-AM inhibited the association between CHL1 and PDCD6. The treatment of cerebellar granule neurons with a cell-penetrating peptide comprising the cell surface proximal 30 N-terminal amino acids of CHL1-ICD inhibited the association between CHL1 and PDCD6 and PDCD6- and CHL1-triggered neuronal survival. These results suggest that PDCD6 contributes to CHL1 functions in the nervous system.

## KEYWORDS

Ca<sup>2+</sup>, cell adhesion molecule, CHL1, nervous system, PDCD6

## 1 | INTRODUCTION

Cell adhesion molecules participate in cell–cell and cell–extracellular matrix interactions contributing to cell proliferation, migration, and differentiation via signal transduction mechanisms.<sup>1–4</sup> Neurons and glial cells express the close homolog of cell adhesion molecule L1 (CHL1) which is implicated in multiple functions during

development and in the adult nervous system.<sup>1,5,6</sup> CHL1 mediates neuronal migration, positioning, and survival, as well as neurite outgrowth, regeneration after injury, and synapse formation, function, and maintenance.<sup>5–16</sup> CHL1-deficient mice show abnormal axonal projections, altered synaptic transmission, deficient long-term potentiation, reduced working memory, abnormal gating of sensorimotor information, stress responses, and altered

Gabriele Loers and Thomas Theis are equally contributing authors.

This is an open access article under the terms of the Creative Commons Attribution-NonCommercial-NoDerivs License, which permits use and distribution in any medium, provided the original work is properly cited, the use is non-commercial and no modifications or adaptations are made.

© 2021 The Authors. *FASEB BioAdvances* published by Wiley Periodicals LLC on behalf of The Federation of American Societies for Experimental Biology

social and exploratory behavior.<sup>9,17–23</sup> In humans, CHL1 mutations are associated with mental retardation, schizophrenia, epilepsy, major depression, and autism spectrum disorders.<sup>24–30</sup>

The extracellular domain of CHL1 binds homophilically with CHL1 molecules on adjacent cells<sup>31</sup> and heterophilically with other molecules such as integrins, contactin 6, extracellular matrix proteins vitronectin and plasminogen activator inhibitor-2, semaphorin 3A, semaphorin 3B, neuropilin 1, hedgehog receptor patched-1, as well as receptor-type protein-tyrosine phosphatase  $\alpha$  and serotonin receptor 2c,<sup>7,11,12,14,32,33</sup> suggesting diverse extracellular interactions of CHL1. The intracellular domain (ICD) of CHL1 also binds to and regulates functions of a wide variety of intracellular molecules, mediates clathrin and neurotransmitter release from clathrin-coated synaptic vesicles,<sup>34</sup> and interacts with heat shock cognate 70 (Hsc70) and other presynaptic chaperones, such as cysteine string protein and the ubiquitous small glutamine-rich tetratricopeptide repeat containing protein, to mediate SNARE (N-ethylmaleimide-sensitive factor attachment protein receptor) complex refolding.<sup>35</sup> Furthermore,  $\beta$ II spectrin binds to CHL1-ICD and both molecules were shown to initiate neuritogenesis.<sup>36</sup>

In this study, we identified programmed cell death 6 (PDCD6), also known as apoptosis-linked gene-2 (ALG-2), as a novel CHL1 interaction partner. PDCD6 is a 22 kDa cytoplasmic protein that belongs to the  $\text{Ca}^{2+}$ -binding penta-EF-hand (PEF) protein family.<sup>37,38</sup> Calcium induces PDCD6 homomultimerization, thereby leading to conformational changes required for binding to functionally relevant interaction partners. Ubiquitously expressed and most prominently in thymus and liver,<sup>39</sup> PDCD6 induces apoptosis in T-cell hybridomas via endoplasmic reticulum stress and causes neuronal cell death during ontogenetic development and in tumors. Some of these functions are mediated by interaction with death-associated protein kinase 1 (DAPk1) or ALG2-interacting protein X (Alix).<sup>38,40–42</sup> PDCD6 contributes to membrane trafficking by interacting with Alix, annexins, tumor susceptibility gene 101 protein, mucolipin-1, and penta-EF-hand domain containing 1 (PEF1).<sup>43–46</sup>

We found that CHL1 and PDCD6 interact and that this association requires  $\text{Ca}^{2+}$  in vitro and in vivo. Furthermore, a peptide derived from CHL1-ICD, which inhibits the association of CHL1 with PDCD6, abolishes CHL1-mediated neuronal survival, but did not affect CHL1-mediated neurite outgrowth in cultured cerebellar neurons or cell migration from cerebellar explants. These findings suggest that CHL1-ICD and PDCD6 together play a major role in preventing apoptosis but do not influence cell migration or neurite growth.

## 2 | MATERIALS AND METHODS

### 2.1 | Animals

CHL1-deficient (CHL1<sup>-/-</sup>) mice,<sup>20</sup> which had been backcrossed onto the C57BL/6J background for more than eight generations, and their age-matched wild-type (CHL1<sup>+/+</sup>) littermates derived from heterozygous parents, as well as C57BL/6J mice were bred and maintained at the animal facility of the Division of Life Sciences at the Nelson Biology Laboratories of Rutgers University and at the University Medical Center Hamburg-Eppendorf. The mice were housed at 25°C on a 12 h-light/12 h-dark cycle with ad libitum access to food and water. Offspring of either sex was used for the preparation of brain homogenates, cryostat brain sections, and primary cell cultures. All animal experiments were approved by the Institutional Animal Care and Use Committee of Rutgers University (protocol no. 09-051) or by responsible authorities of the State of Hamburg (Behörde für Wissenschaft und Gesundheit, Amt für Gesundheit und Verbraucherschutz, Lebensmittelsicherheit und Veterinärmedizin; animal permit numbers ORG 679 Morph and ORG 1022).

### 2.2 | Antibodies and chemical reagents

Polyclonal goat antibody (#AF2147) against CHL1 was purchased from R&D Systems. Rabbit polyclonal PDCD6 antibody (#12303-1-AP) was purchased from Proteintech. Rabbit polyclonal HSP60 antibody (#4870S) was purchased from Cell Signaling Technology. Rabbit monoclonal PEF1 antibody (#ab137127) was purchased from Abcam. Non-immune rabbit IgG control (#AB105C) was purchased from R&D Systems. Mouse GFAP antibody (clone GA5, #MAB-360) and mouse tubulin  $\beta$ -III antibody (clone TU-20, #MAB1637) were purchased from Millipore. Secondary antibodies, including anti-goat IgG (#705-035-147) and anti-rabbit IgG (#711-035-152) conjugated to horseradish peroxidase, and anti-mouse IgG conjugated with Alexa Fluor 647 (#715-605-150) were purchased from Jackson ImmunoResearch. The following reagents were purchased from Sigma-Aldrich unless stated otherwise: secondary antibodies, including anti-goat IgG conjugated with Alexa Fluor 568 (#A11057), anti-rabbit IgG conjugated with Alexa Fluor 488 (#A21206), goat polyclonal anti-biotin antibody (#31852), protein A/G magnetic beads (#PI88802), Novex™ iBlot™ 2 PVDF regular stacks (#IB24001), calcein-AM (#C1430), Hank's Balanced Salt Solution (HBSS, #14175095), Neurobasal A (#10888022), B27 supplement (#17504044), and Opti-MEM medium (#31985070) were purchased from Thermo Fisher Scientific. Ethylene glycol-bis( $\beta$ -aminoethyl)-N,N,N',N'-tetraacetic acid (EGTA, #324626), 2-(4-amidinophenyl)-6-indolecarbamidi

ne dihydrochloride (DAPI, #D9542), RIPA buffer (#R0278), Triton X-100 (#T8787), Tween 20 (#P1379), glutaraldehyde (#G6257), poly-L-lysine hydrobromide (PLL, #P1274), isopentane (#270342), propidium iodide (#P4170), and Duolink in situ proximity ligation assay reagents including anti-rabbit minus probe (#DUO92005), and anti-goat plus probe (#DUO92003), and orange detection reagents (#DUO92007). 1,2-Bis(2-aminophenoxy)ethane-N,N,N',N'-tetraacetic acid tetrakis(acetoxymethyl ester) (BAPTA-AM, #2787/25) was purchased from Tocris. Proteinase inhibitor cocktail (#5892791001) was purchased from Roche. Nickel-NTA agarose beads (#30210) were purchased from Qiagen. Enhanced chemiluminescence (ECL) western blot substrate (#32106) was purchased from Pierce. The mounting reagent Aquapoly/mount (#18606) was purchased from Polysciences. Cloning and production of recombinant his-tagged intracellular domains of CHL1 (CHL1-ICD) and NCAM140 (NCAM-ICD) have been described.<sup>34,47</sup> CHL1Fc, containing the extracellular domain of CHL1 fused to Fc from human IgG, was prepared as described.<sup>48</sup>

### 2.3 | Affinity chromatography and mass spectrometry

Twenty brains of 3- to 4-month-old C57BL/6J mice of both genders were dispersed in homogenization buffer (0.32 M sucrose, 50 mM Tris/HCl, pH 7.5, 1 mM CaCl<sub>2</sub>, 1 mM MgCl<sub>2</sub>; 3 ml per brain) using a Dounce homogenizer (20 strokes). This and all subsequent steps were carried out at 4°C. The homogenate was centrifuged at 1000 g for 15 min and the resulting supernatant was further centrifuged at 17,000 g for 30 min. For affinity chromatography, the 17,000 g supernatant was taken as soluble protein fraction containing cytoplasmic proteins.

Recombinant his-tagged CHL1-ICD or NCAM-ICD was immobilized on CNBr-activated Sepharose 4B (#17-0430-01; GE Healthcare Europe) according to the manufacturer's instructions. The crude homogenate and cytoplasmic fractions were applied to the columns with immobilized CHL1-ICD or NCAM-ICD overnight at 4°C at a flow rate of 0.1 ml/min. After washing the columns with 10 ml of homogenization buffer (0.3 ml/min), bound proteins were eluted with 100 mM glycine, pH 2.3 (0.3 ml/min). The eluted fractions were collected and immediately neutralized with 1 M Tris/HCl, pH 8.0. After ultrafiltration and reducing the volume of the eluates using Amicon Ultra 5 kDa MWCO tubes (#Z648019; Merck Millipore), eluted proteins were separated on a 8%–20% SDS gradient gel (#4561096; Bio-Rad). After staining the gel with colloidal Coomassie Blue (#A152.1; Carl Roth), stained protein bands were cut out and subjected to nano-electrospray mass spectrometry using a QTOF II instrument (Micromass®, Waters Corporation) as described.<sup>49</sup>

The MS/MS spectra obtained by collision-induced fragmentation of the peptides were evaluated both manually and by the Mascot MS/MS ion search algorithm (Matrix Sciences).

### 2.4 | Western blot analysis, immunoprecipitation, and pull-down assay

Western blot analysis, immunoprecipitation, and pull-down assay were performed as described.<sup>50,51</sup> Briefly, for immunoprecipitation, brains from CHL1<sup>-/-</sup> or CHL1<sup>+/+</sup> littermate mice (3 day old, 1 month old, or 6 month old) were homogenized with a glass homogenizer in RIPA buffer (150 mM NaCl, 1.0% IGEPAL® CA-630, 0.5% sodium deoxycholate, 0.1% SDS, 50 mM Tris, pH 8.0) containing proteinase inhibitor cocktail. Tissue debris was removed by centrifugation at 1000 g and 4°C for 10 min. The pre-cleared supernatant (1 mg protein/ml) was incubated with 2 µg PDCD6 antibody or non-immune rabbit IgG (as negative control). Then, 20 µl of magnetic protein A/G beads was added to the samples and incubated overnight at 4°C. After washing four times with RIPA buffer, protein complexes were eluted from the beads with SDS NuPAGE™ LDS sample buffer (#NP0007, Thermo Fisher Scientific) and subjected to SDS-PAGE followed by western blot analysis. In the pull-down experiment, the pre-cleared supernatant was incubated with 50 µg his-tagged CHL1-ICD. Then, Ni-NTA agarose beads were added to pull down his-tagged proteins, incubated for 4 h at 4°C with agitation, and beads were collected by centrifugation at 1000 g and 4°C for 5 min. After washing three times with RIPA buffer and once with PBS, the collected protein complexes were treated with sample buffer, and subjected to SDS-PAGE and western blot analysis. Immunoreactive bands were visualized using ECL detection reagent and recorded with the Odyssey Fc imaging system. The intensities of immunopositive bands were quantified with Image Studio lite version 5.2 software (Li-COR, Lincoln, NE, USA).

### 2.5 | Tissue preparation, immunohistochemistry, and proximity ligation assay

Tissue preparation, immunohistochemistry, and proximity ligation assay were performed as described.<sup>32</sup> Transcardial perfusion of 3-day-old and 6-month-old CHL1<sup>-/-</sup> and CHL1<sup>+/+</sup> littermate mice was performed with saline containing 10 U/ml heparin and then with 4% formaldehyde in 0.1 M phosphate buffer, pH 7.3. Brains were dissected and post-fixed overnight at 4°C with 4% formaldehyde in 0.1 M phosphate buffer, pH 7.3. The brains were then washed once in phosphate-buffered saline, pH 7.3 (PBS) and incubated in 10%, 20%, and 30% sucrose solution for 24 h each at 4°C until brains collected at the

tube bottom, frozen by immersion for 2 min in isopentane pre-cooled to  $-80^{\circ}\text{C}$ , and stored at  $-80^{\circ}\text{C}$  until use. Serial sagittal 25- $\mu\text{m}$ -thick cerebellar sections were cut in an OTF5000 cryostat (Bright Instruments, UK) and collected on Superfrost Plus glass slides (#12-550-15, Thermo Fisher Scientific). Cerebellar granule cells and astrocytes cultured on poly-L-lysine (PLL, 0.01%) coated coverslips were fixed in 4% formaldehyde in 0.1 M phosphate buffer, pH 7.3, for 30 min at room temperature, and then washed two times with PBS before blocking. For immunostaining and proximity ligation assay (PLA), the sections (consecutive or those with 625  $\mu\text{m}$  spacing) or fixed cerebellar granule cells and astrocytes were blocked with PBS containing 0.2% Triton X-100 and 5% normal donkey serum for 1 h at room temperature. Mixtures of goat CHL1 antibody (1:100) and rabbit PDCD6 antibody (1:100) and thereafter of donkey Alexa Fluor 555-conjugated anti-goat IgG and Alexa Fluor 488-conjugated anti-rabbit IgG antibodies (1:500) were used for the detection of CHL1 and PDCD6. In the proximity ligation assay, mixtures of goat CHL1 (1:100) and rabbit PDCD6 antibodies (1:100) as well as Duolink anti-goat PLA probe PLUS and Duolink anti-rabbit PLA probe MINUS were used. For staining cells transfected with CHL1 peptides, goat anti-biotin antibody (1:1,000) and thereafter of donkey Alexa Fluor 488-conjugated anti-goat IgG antibody (1:500) were used for the detection of biotinylated proteins. Nuclei were stained with DAPI for 10 min at room temperature. Coverslips were mounted with aqueous fluorescent mounting solution (#HC08; Merck) and confocal images were taken with a Carl Zeiss LSM 800 confocal laser scanning microscope in sequential mode with a 63 $\times$  objective and 0.85 numerical aperture and processed with Zen software (Carl Zeiss, Germany). For visualizing 3D reconstruction images resulting from the PLA, Z-stack of 12 consecutive images were taken at 1  $\mu\text{m}$  intervals from cerebellum or pons of 3-day-old mice.

The PLA signal, shown as red fluorescent puncta, was semi-automatically counted in the region of interests (in vitro: cell soma; in vivo: tissue area) using the ImageJ software (National Institutes of Health). In brief, the contrast/brightness threshold was set on the “Li” function. Background noise was removed using despeckle, erode, and dilate functions of ImageJ. Then, watershed ImageJ function was run on the processed images to improve accuracy. Regions of interest were selected, and puncta were counted using the analyze particles function of ImageJ.

## 2.6 | CHL1-ICD peptide design and transfection of cultured cerebellar granule cells

The synthetic biotin and TAT (GRKKRRQRRR) sequence-carrying CHL1 peptides P1 (Biotin-GRKKRRQRRRKRNRGGKYSVKEKEDLHPDPEVQSAKDETF), P2 (Biotin-GRK

KRRQRRRKDETFGEYSDSDEKPLKGSRLSLNRNMQPT), P3 (Biotin-GRKKRRQRRRNMQPTESADSLVEYGEGDQ SIFNEDGSFIG), and P4 (Biotin-GRKKRRQRRRGSFIGA YTGAKKEKGSVESNGSSTATFPLRA) were obtained from GenScript (Piscataway, NJ, USA) or Schafer-N (Denmark, Netherlands). For the transfection of CHL1 peptides into cerebellar granule cells, peptide stock solutions (1 mM in Opti-MEM or HBSS) were prepared and added to the cultures at time points and concentrations as indicated.

## 2.7 | Astrocyte culture

Astrocytes from brains of 0- to 2-day-old wild-type C57BL6/J mice of either sex were prepared and cultured with minor modifications as described.<sup>52</sup> In brief, after removing meninges, brains were cut into 3–5 mm diameter pieces, washed them three times with HBSS (Gibco, cat# 14025-092), and incubated in 0.25% Trypsin-EDTA (Gibco, cat# 25200-056). We then washed the pieces three times with HBSS, added DNase I solution (HBSS + 0.05% DNase I + 0.25% glucose + 0.8 mM  $\text{MgCl}_2$ ), and mechanically dissociated the cells with a 1 ml micropipette. The mixed glial cells were cultured for at least 1 week at  $37^{\circ}\text{C}$  and 5%  $\text{CO}_2$  in DMEM (Gibco, cat# 11965-092) containing 10% horse serum (Genini, cat# 100-508, lot# E18H00H) and 10% fetal bovine serum (Genini, cat# 900-108, lot# A246) on PLL-coated 6-well plates until they had reached confluence. Next, we separated the monolayer of astrocytes from other glial cells by shaking the plates at 200 rpm for 2 h at room temperature, discarded the medium, treated the astrocytes for 5 min at  $37^{\circ}\text{C}$  with 0.25% Trypsin-EDTA, diluted in DMEM with 10% horse serum and 10% fetal bovine serum, seeded them on PLL-coated glass cover slips ( $1 \times 10^6$  cells/ml), and maintained them for 3 days in culture.

## 2.8 | Cell survival, neurite outgrowth, and neuronal survival

Primary cerebellar granule cells were prepared from 6- to 8-day-old CHL1<sup>+/+</sup> or CHL1<sup>-/-</sup> mice of either sex.<sup>53</sup> Dissociated cells were resuspended in serum-free X-1 medium (Neurobasal-A medium supplemented with 1% penicillin/streptomycin, 0.1% bovine serum albumin, 10  $\mu\text{g}/\text{ml}$  insulin, 4 nM L-thyroxine, 100  $\mu\text{g}/\text{ml}$  transferrin holo, 30 nM Na-selenite, 2 mM L-glutamine, and 0.5% B27) and cell numbers were counted. The cell culture plates or coverslips were coated with 0.01% PLL. For cell survival assay, cells were diluted to  $1 \times 10^6$  cells/ml and plated into 48-well plates (250  $\mu\text{l}/\text{well}$ ). For neurite outgrowth experiments, cells were diluted to  $1 \times 10^5$  cells/

ml and plated into 48-well plates (250  $\mu$ l/well). For immunostaining, cells were diluted to  $2.5 \times 10^5$  cells/ml and plated onto glass coverslips in 24-well plates (500  $\mu$ l/well).

For cell death analyses, cerebellar granule cells were cultured for 16 h in a serum-free medium at 37°C in 5% CO<sub>2</sub> and 90% humidity, then treated with CHL1Fc (5  $\mu$ g/well) and 1  $\mu$ M CHL1 peptides P1, P2, P3, or P4 for 30 min, followed by the application of 10  $\mu$ M H<sub>2</sub>O<sub>2</sub> to induce cell death. Cells were maintained for further 32 h, and live and dead cells were determined by staining with calcein-AM and propidium iodide (each 1  $\mu$ g/ml) for 30 min at 37°C. Live imaging of cerebellar granule cells was performed using a Carl Zeiss AxioObserver.A1 microscope with a 20 $\times$  objective and AxioVision 4.6 software. Numbers of live cells and dead cells were determined from four images of three wells per condition (15 images/condition) using ImageJ software (National Institutes of Health) as described.<sup>53</sup> Cell numbers of live and dead cells were averaged for each image, and the percentage of live cells was calculated. Experiments were performed at least three times.

Neurite outgrowth measurements were performed as described.<sup>53</sup> Cerebellar granule cells were allowed to settle for 30 min and then treated with CHL1Fc (5  $\mu$ g) and 1  $\mu$ M CHL1 peptides P1, P2, P3, or P4. Neurons were maintained for 24 h at 37°C in 5% CO<sub>2</sub> and 90% humidity, fixed with 2.5% glutaraldehyde for 1 h at 22°C, and stained with 1% toluidine blue and 0.1% methylene blue in 1% sodium tetraborate. Neurites were imaged and quantified using a Carl Zeiss AxioObserver.A1 microscope with a 20 $\times$  objective and AxioVision 4.6 software. The neurite lengths were measured from the edge of the cell body to the end of the process, taking into account only neurites with a length equal to or greater than the diameter of the cell soma from which they originated and only from those that showed no contact with other neurites or cell bodies. For each experiment at least 100 cells were counted per condition and experiments were repeated two times.

Cerebellar explants were prepared from 6- to 7-day-old CHL1<sup>+/+</sup> or CHL1<sup>-/-</sup> mice.<sup>54</sup> In brief, cerebella were consecutively forced through Nitrex nets with pore sizes of 300, 200, and 100  $\mu$ m, and explants were plated on 12 mm glass coverslips coated with 0.01% PLL and maintained for 16 h in 80  $\mu$ l culture medium containing 20% horse serum. The coverslips with explants were placed into 24-well plates with 500  $\mu$ l serum-free medium, treated with 10  $\mu$ g CHL1Fc and 1  $\mu$ M CHL1 peptides P1, P2, P4, or P4. After 32 h, the explants were fixed and stained. Migration of neurons was determined from at least 12 explants per treatment. To quantify the number of migrating cells, all cells outside of the explant border were counted using the

AxioVision software 4.6 (Zeiss). Experiments were carried out independently at least three times.

## 2.9 | Statistical analysis

All experiments were performed and analyzed in a blinded manner with the investigators not knowing which cultures were treated with which compound. Student's *t*-test was used to compare the results from CHL1<sup>-/-</sup> and CHL1<sup>+/+</sup> mice and ANOVA was used to compare the data of cell culture experiments. A *p* value below 0.05 was considered to be statistically significant.

## 3 | RESULTS

### 3.1 | Identification of PDCD6 as a novel interaction partner of CHL1

To identify interaction partners of CHL1-ICD, we did affinity chromatography using immobilized CHL1-ICD and a brain subfraction containing soluble cytoplasmic proteins. Immobilized neural cell adhesion molecule NCAM-ICD, a member of the Ig superfamily of adhesion molecules, served as control. Bound proteins were eluted, separated by gel electrophoresis, and visualized by colloidal Coomassie brilliant blue staining. To identify proteins that specifically interact with CHL1 and not also with other adhesion molecules, we used mass spectrometry to assess protein bands detectable in the eluate from the CHL1-ICD column, but not in the eluate from the NCAM-ICD column. In the eluates from the CHL1-ICD column, we matched tryptic peptides in a ~22 kDa protein band with MS/MS spectra of 1443.6, 1357.6, 1341.6, and 985.4 Da precursor masses (detected as doubly charged ion at *m/z* = 721.8, 678.8, 670.8, and 492.7) with tryptic peptides AGVNFSEFTGVWK (1441.7 Da; aa 78–90), LSDQFHDILIR (1356.7 Da; aa 126–136), YITDWQNVFR (1341.6 Da; 91–100), and SIISMFDR (968.5 Da with methionine oxidized to methionine sulfoxide resulting in a mass of 984.5 Da; 67–74) of mouse PDCD6 (UniProtKB/Swiss-Prot accession number: P12815; 21,854 Da).

### 3.2 | Expression of CHL1 and PDCD6 in the cerebellum and whole brain

To study the interactions between CHL1 and PDCD6, we analyzed the expression pattern of CHL1 and PDCD6 in mouse cerebellum and pons at three different ages by western blot analysis. The cerebellum was chosen since we have used it in many of our studies. Cerebellar granule

cells were also used for cell culture experiments in the present study. The pons was used because it can be removed from the brain leaving the rest of the brain intact for other studies. Three-day-old CHL1<sup>+/+</sup> mice expressed more CHL1 than brains of 1-month-old and 6-month-old mice, whereas the expression of PDCD6 was similar at all ages (Figure 1A,B). CHL1 deficiency did not affect the expression levels of PDCD6 at these ages (Figure 1A–C). CHL1 is more highly expressed in the cerebellum of 3-day-old mice than in 1-month-old and 6-month-old mice (Figure 1D–F). The expression levels of PDCD6 in the cerebellum are similar at these three ages and do not differ between CHL1<sup>+/+</sup> and CHL1<sup>-/-</sup> mice (Figure 1D–F).

### 3.3 | association of CHL1 with PDCD6 depends on Ca<sup>2+</sup>

Since brains of 3-day-old wild-type mice show the highest CHL1 expression, we performed co-immunoprecipitation

experiments using brain homogenate of 3-day-old mice and rabbit anti-PDCD6 antibody and rabbit non-immune IgG (as negative control). Western blot analysis of the immunoprecipitates showed CHL1 as a band of approximately 185 kDa and PDCD6 as a band of approximately 20 kDa in the PDCD6 immunoprecipitate, but not in the immunoprecipitate obtained with the non-immune IgG (control) (Figure 2A). This result suggests that PDCD6 associates with CHL1.

To investigate if PDCD6 associates with the CHL1-ICD, we did pull-down experiments using brain homogenate of a 3-day-old CHL1<sup>+/+</sup> mouse. We purified recombinant His-tagged CHL1-ICD protein, containing the intracellular domain of mouse CHL1, from bacteria as described.<sup>36</sup> CHL1-ICD or PBS as a vehicle control was incubated with brain homogenate and then with Ni-NTA beads to pull-down CHL1-ICD via its His-tag. Western blot analysis using PDCD6 antibody revealed a PDCD6 immunopositive band at approximately 20 kDa in CHL1-ICD precipitates, while no band was

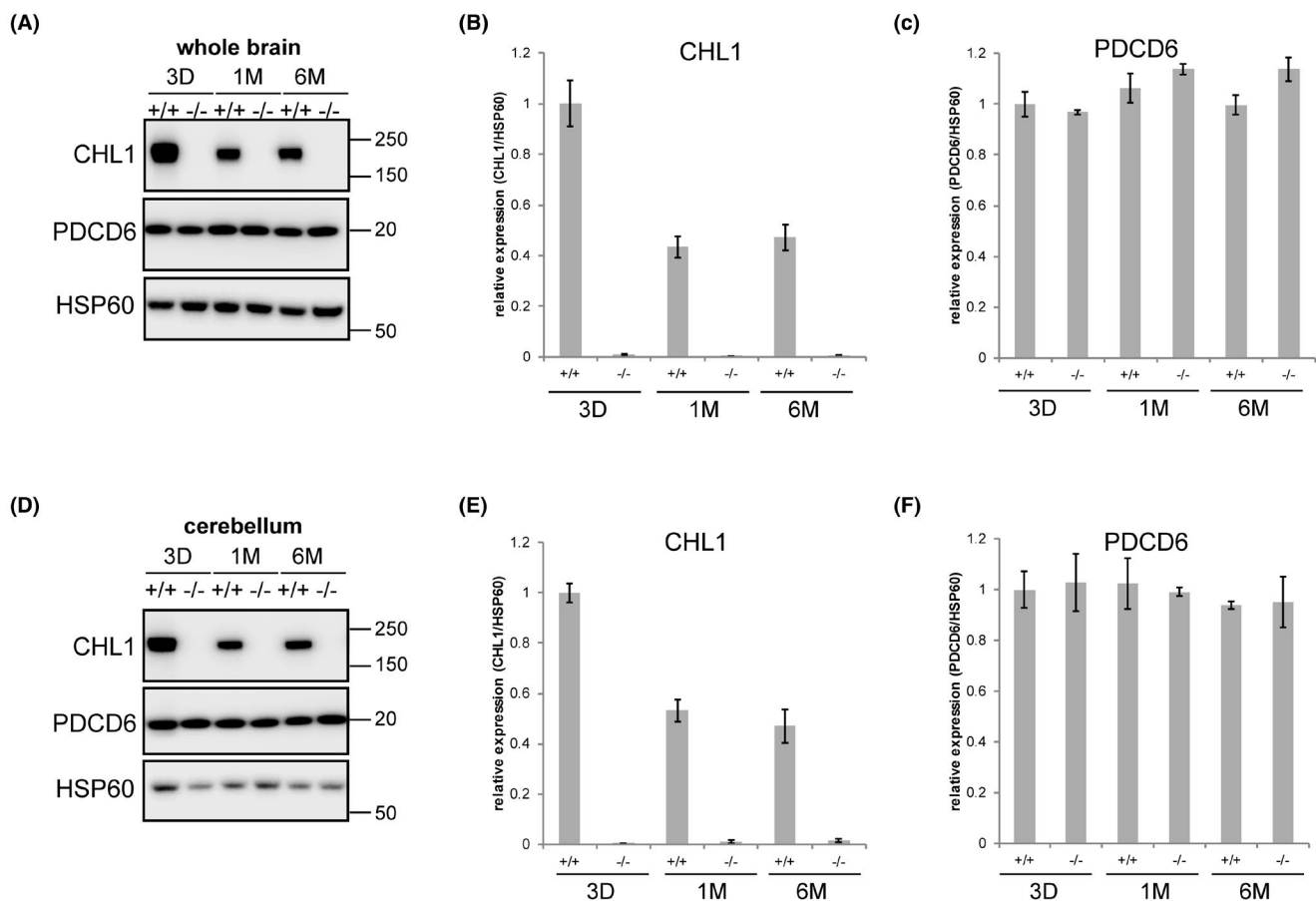


**FIGURE 1** Expression of CHL1 and PDCD6 in whole brain and cerebellum during development. Whole brains and cerebella from age-matched wild-type (+/+) and CHL1-deficient (-/-) littermates at three ages (3 days: 3D, 1 month: 1M, and 6 months: 6M) were used. The whole brains (A) and cerebella (D) were dissected, homogenized, and analyzed for the expression of CHL1, PDCD6, and HSP60 (loading control) by western blot analysis. (B, C, E, F) Quantification of the relative expression levels of CHL1 (B, E) and PDCD6 (C, F) normalized to HSP60. Data show average values  $\pm$  SEM. For the analysis, three brains or cerebella per genotype and age were used

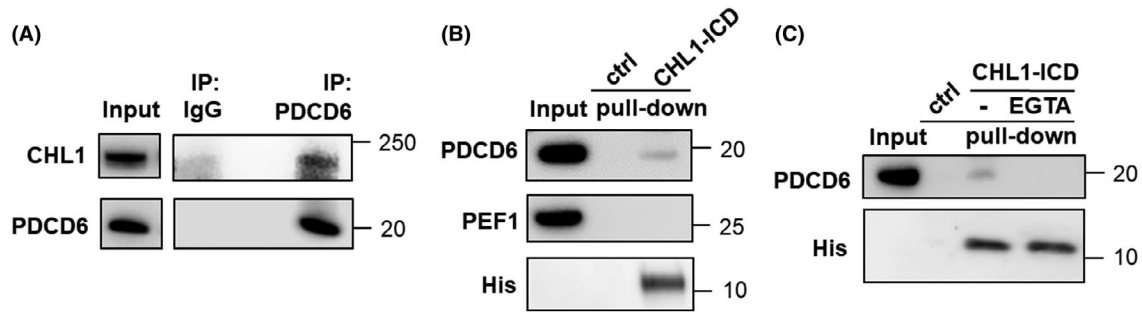


**FIGURE 2** The association of CHL1 with PDCD6 depends on  $\text{Ca}^{2+}$ . (A) Homogenates of brains from 3-day-old  $\text{CHL1}^{+/+}$  mice were subjected to immunoprecipitation (IP) with rabbit IgG control (ctrl) or PDCD6 antibody (PDCD6) followed by western blot analysis using antibodies against CHL1 and PDCD6. (B) PBS control (ctrl) or His-tagged CHL1-ICD was incubated with brain homogenates of 3-day-old  $\text{CHL1}^{+/+}$  mice followed by pull-down with Ni-NTA beads. Brain homogenates (input) and immunoprecipitates were probed by western blot analysis with antibodies against PDCD6, His-tag, and PEF1 (as negative control). (C) PBS control (ctrl) or his-tagged CHL1-ICD was incubated with brain homogenates of 3-day-old  $\text{CHL1}^{+/+}$  mice containing PBS alone (–) or PBS and 0.5 mM EGTA (EGTA), followed by pull-down with Ni-NTA beads. Brain homogenates (input) and precipitates were probed by western blot using antibody against PDCD6. Precipitates were probed by western blot analysis using antibody against His-tag for the quantification of CHL1-ICD. Experiments were performed independently three times

detected in control immunoprecipitates lacking CHL1-ICD. PEF1, also belonging to the PEF protein family like PDCD6, was not co-immunoprecipitated, as the PEF1 antibody did not show any immunopositive bands at approximately 25 kDa (Figure 2B). Since  $\text{Ca}^{2+}$  has been reported to be required for the binding of PDCD6 with other proteins,<sup>43,44,46</sup> 0.5 mM EGTA was added to the incubation mixture of CHL1-ICD and mouse brain homogenate to chelate residual  $\text{Ca}^{2+}$  in the pull-down experiment. Western blot analysis of the CHL1-ICD precipitates showed that the PDCD6 band at approximately 20 kDa was not detectable in the presence of EGTA (Figure 2C). Western blot analysis confirmed equal pull-down of CHL1-ICD in the presence and absence of EGTA, showing that the reduced levels of PDCD6 in the samples are due to the presence of EGTA and not due to reduced levels of CHL1-ICD pulled-down with the beads (Figure 2C).

These results indicate that the interaction of PDCD6 with CHL1-ICD depends on  $\text{Ca}^{2+}$ .

### 3.4 | Close interaction between CHL1 and PDCD6 in cerebellum and pons

To assess whether CHL1 and PDCD6 are in close contact, we did proximity ligation assays to detect close molecular interactions with high sensitivity and specificity by amplifying fluorescent signals from a pair of oligonucleotide-labeled secondary antibodies. Such signals indicate a close proximity of the two proteins within 40 nm or less.<sup>12,32</sup> In the cerebellum, we observed fluorescent spots in the emerging molecular

layer, Purkinje cell layer and internal granular layer of 3-day-old  $\text{CHL1}^{+/+}$  mice, and Purkinje cell layer of 6-month-old  $\text{CHL1}^{+/+}$  mice, but not in 3-day-old or 6-month-old  $\text{CHL1}^{-/-}$  mice (Figure 3A–C,G,H). Fluorescent spots were also present in the pons of 3-day-old or 6-month-old  $\text{CHL1}^{+/+}$  mice, but not of  $\text{CHL1}^{-/-}$  mice (Figure 3D–F,I,J). Signal quantification showed approximately 50 fluorescent spots per  $10^4 \mu\text{m}^2$  area in the cerebellum of 3-day-old and 6-month-old  $\text{CHL1}^{+/+}$  mice (Figure 3C,H). Comparison of the pons 3-day-old  $\text{CHL1}^{+/+}$  mice and 6-month-old  $\text{CHL1}^{+/+}$  mice showed about 50 and 30 fluorescent spots in 3-day-old and 6-month-old  $\text{CHL1}^{+/+}$  mice, respectively (Figure 3F,J). Confocal 3D reconstruction images of  $\text{CHL1}^{+/+}$  cerebellum and pons showed the distribution of fluorescent signals more clearly than the single stack images (Figure 3B,E), suggesting close proximity of CHL1 and PDCD6 in developing cerebellum and pons which would allow direct protein interaction.

### 3.5 | CHL1 and PDCD6 co-localize in astrocytes and neurons

Since both neurons and astrocytes express CHL1 and PDCD6, we confirmed the co-localization of CHL1 and PDCD6 in cultured cerebellar neurons and astrocytes by double immunostaining (Figure 4A–D). Both cell types express PDCD6 and CHL1, but CHL1 expression was strongest at cell surfaces of granule cell neurons, along their neurites, and on the surface of astrocytes. Astrocytes and neurons from  $\text{CHL1}^{-/-}$  mice did not show

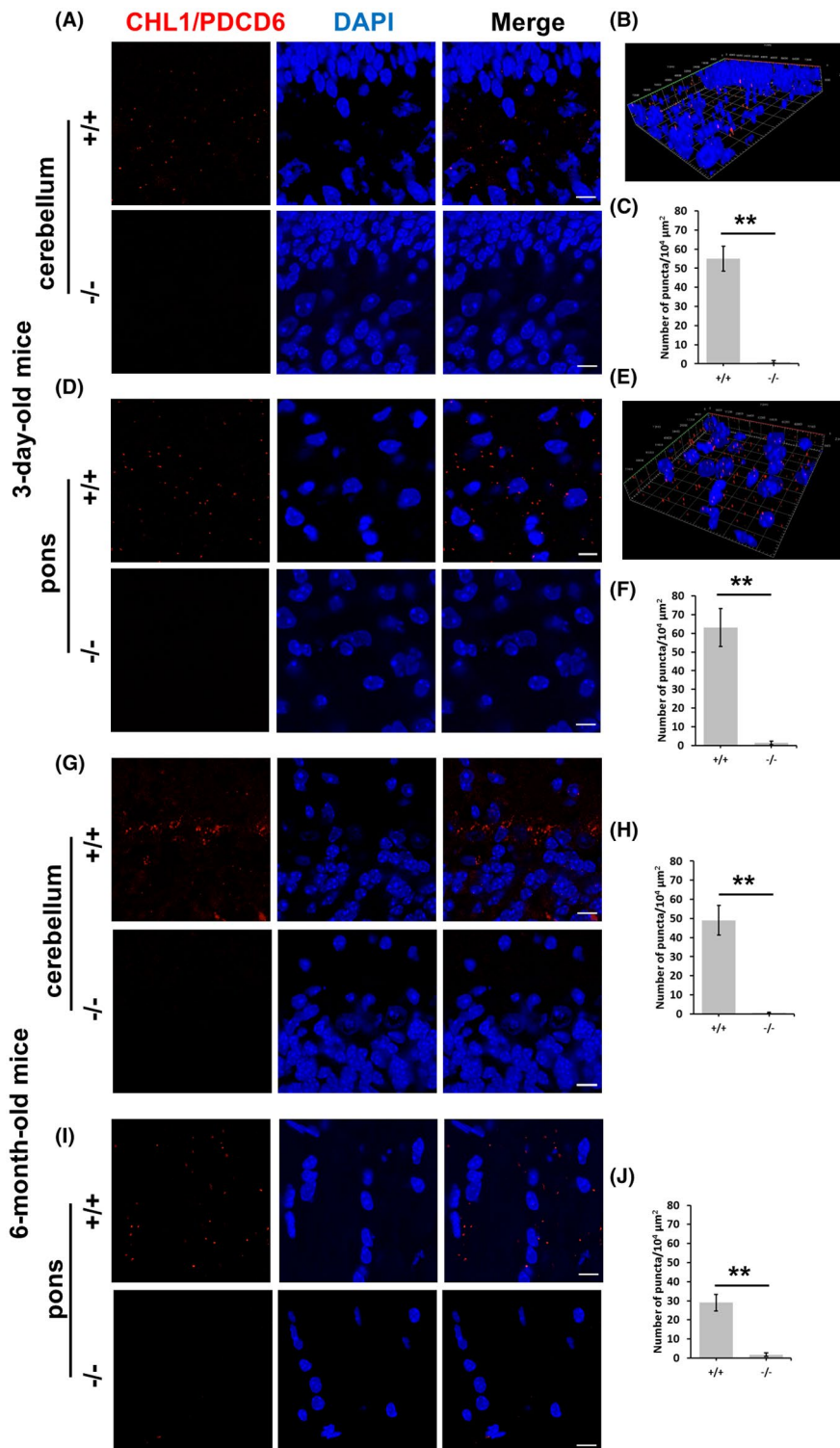


**FIGURE 3** Close proximity of CHL1 and PDCD6 in the cerebellum and pons of 3-day-old and 6-month-old mice. Brain slices from 3-day-old and 6-month-old mice were used for proximity ligation assay with antibodies against CHL1 and PDCD6. (A, D) Representative confocal images for cerebellum (A) and pons (D) from three 3-day-old  $\text{CHL1}^{+/+}$  and  $\text{CHL1}^{-/-}$  mice are shown. (B, E) 3D reconstruction images of  $\text{CHL1}^{+/+}$  cerebellum (B) and pons (E) from 2D merged images in (A) and (D), respectively. (C, F) Quantification of average numbers of puncta in the whole area of each image ( $10^4 \mu\text{m}^2$ ) in the cerebellum (C) and pons (F) of 3-day-old  $\text{CHL1}^{+/+}$  and  $\text{CHL1}^{-/-}$  mice. Data are presented as the mean  $\pm$  SEM from three mice (10 sections per mouse brain). (G, I) Representative confocal images for cerebellum (G) and pons (I) from three 6-month-old  $\text{CHL1}^{+/+}$  and  $\text{CHL1}^{-/-}$  mice are shown. (H, J) Quantification of average numbers of puncta in the whole area of each image ( $10^4 \mu\text{m}^2$ ) in the cerebellum (H) and pons (J) of 6-month-old  $\text{CHL1}^{+/+}$  and  $\text{CHL1}^{-/-}$  mice. Data are presented as the mean  $\pm$  SEM from three mice (10 sections per mouse brain). Red spots of intense fluorescent signals indicate the close proximity of CHL1 and PDCD6. Nuclei were stained with DAPI (blue). Scale bars, 10  $\mu\text{m}$ .  $**p < 0.01$  with Student's *t*-test

fluorescent signals for CHL1 (data not shown). To determine the level of co-localization, the Pearson's coefficient was determined. In neurons, the Pearson's coefficient was  $r = 0.523$  and in astrocytes the Pearson's coefficient was  $r = 0.706$ , showing that the signals are moderately correlated and that CHL1 and PDCD6 are in close contact.

### 3.6 | Close proximity of CHL1 and PDCD6 in astrocytes and neurons

The proximity ligation assay showed that CHL1 and PDCD6 localize with each other at a distance of 40 nm or less. Higher numbers of red spots were observed in

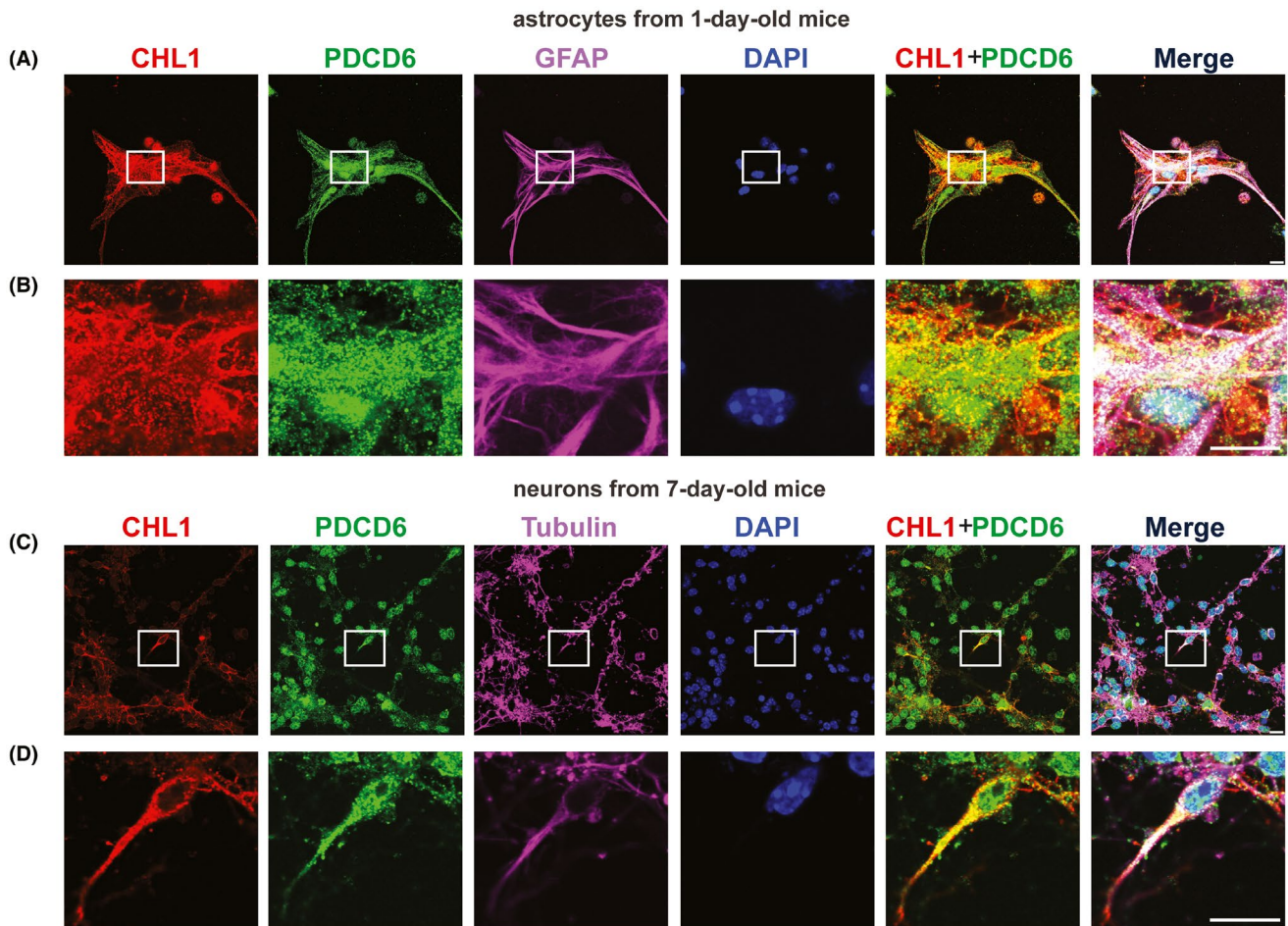


**FIGURE 4** Co-localization of CHL1 and PDCD6 in cerebellar astrocytes and neurons. (A–D) Cultures of astrocytes from 1-day-old wild-type mice (A, B) and cerebellar neurons from 7-day-old wild-type mice (C, D) were maintained for 3 days and used for immunostaining of cultured cells. Representative confocal images of triple immunofluorescence staining for CHL1 (red), PDCD6 (green), and tubulin or GFAP (purple) from three mice per group. The nuclei were stained with DAPI (blue). Scale bars, 10  $\mu\text{m}$ . Boxes indicate the area shown in the magnifications

astrocytes from CHL1<sup>+/+</sup> mice while very few red spots were detectable in astrocytes from CHL1<sup>-/-</sup> littermates (Figure 5A). Quantification of signals showed approximately 15 fluorescent spots in each CHL1<sup>+/+</sup> astrocyte when compared with approximately one fluorescent spot in CHL1<sup>-/-</sup> astrocytes (Figure 5D). About 0.2 spots were present per CHL1<sup>+/+</sup> neuron and less than one fluorescent spots in CHL1<sup>-/-</sup> neurons (Figure 5B,E). Neurons had fewer fluorescent spots than astrocytes (Figure 5D,E). This may be due to the larger area covered by flat monolayer astrocytes as compared to granule neurons, which have a small cell body and diffusely distributed neurites that have a filigree appearance. These results confirm the close proximity of CHL1 and PDCD6 in both neurons and astrocytes suggesting that the two proteins are directly interacting or present in a tight complex.

### 3.7 | The N-terminus of the CHL1-ICD mediates the association of CHL1 with PDCD6

To identify the domain of CHL1-ICD required for CHL1 association with PDCD6, we synthesized four CHL1 peptides comprising the entire sequence of the CHL1-ICD from the surface membrane-close N-terminus to the membrane-distant C-terminus (Figure 6A). The peptides were coupled with biotin at the N-terminus and contained the TAT sequence to monitor the transfection efficiency of the cerebellar granule neurons. The peptide sequence required for the association of CHL1 with PDCD6 should compete with endogenous CHL1 for binding to PDCD6, thereby reducing the association between the two proteins.

All four CHL1-ICD peptides entered cells with high and similar efficacy as shown by immunofluorescence

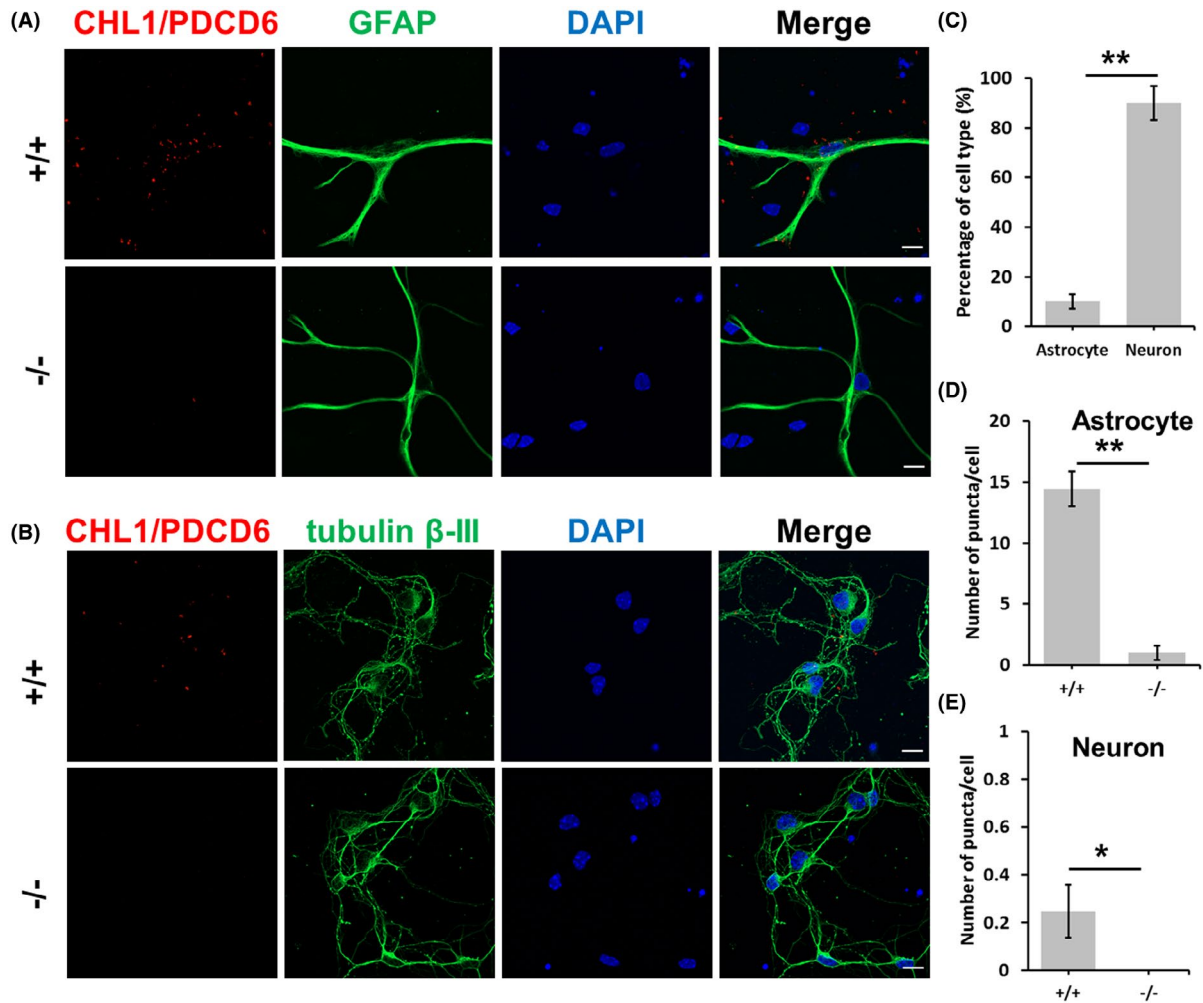


**FIGURE 5** Close proximity of CHL1 and PDCD6 in cerebellar astrocytes and neurons. Cultures of dissociated cerebellar cells from 7-day-old CHL1<sup>+/+</sup> and CHL1<sup>-/-</sup> mice were maintained for 3 days and used for proximity ligation assay with antibodies against CHL1 and PDCD6. (A, B) Representative confocal images for astrocytes (A) stained with GFAP (green) and neurons (B) stained with tubulin β-III (green) are shown. Red spots of intense fluorescent signals indicate the close interaction between CHL1 and PDCD6. The nuclei were stained with DAPI (blue). Scale bars, 10 μm. (C) Quantification of the percentage of astrocytes and neurons in CHL1<sup>+/+</sup> cerebellar cell cultures. (D, E) Quantification of average numbers of puncta per astrocyte (D) or neuron (E) in the CHL1<sup>+/+</sup> and CHL1<sup>-/-</sup> groups. Data are presented as the mean ± SEM from three independent experiments. Fourteen images were evaluated and more than 100 cells (ctrl: 120 cells, P1: 154 cells, P2: 158 cells, P3: 155 cells, P4: 161 cells) were counted from each group. To quantify the PLA signal in neurons, puncta in tubulin β-III stained cells and processes were counted, for astrocytes puncta in GFAP stained cells and their protrusions were counted. Confocal images are shown as representative results out of three mice per group. \**p* < 0.05; \*\**p* < 0.01 with Student's *t*-test

staining of the biotin tags. Vehicle control transfected cells did not show any signal (Figure 6B). CHL1 peptides required for the association with PDCD6 should reduce the interaction of endogenous CHL1 with PDCD6 and show less proximity ligation signal. Only CHL1 peptide P1 reduced the number of fluorescent spots (about eight spots per cell) when compared with control or other peptides (about 15 spots per cell) (Figure 6C,D). This result suggests that the 30 N-terminal amino acids closest to the surface membrane are required for the association of CHL1 and PDCD6 and mediate direct interactions between the two proteins.

### 3.8 | CHL1-ICD peptide P1 reduces the survival of cerebellar granule neurons, but does not influence the neurite outgrowth and neuronal migration

To determine if CHL1-ICD peptides affect survival rate, neurite outgrowth, and migration of cerebellar granule cells, we measured cell death, cell migration, and neurite outgrowth in cultures of dissociated cerebellar granule neurons and cerebellar explants. In unstressed neurons, viabilities of CHL1<sup>-/-</sup> and CHL1<sup>+/+</sup> cells in both control and CHL1 peptide-transfected cells were similar. In

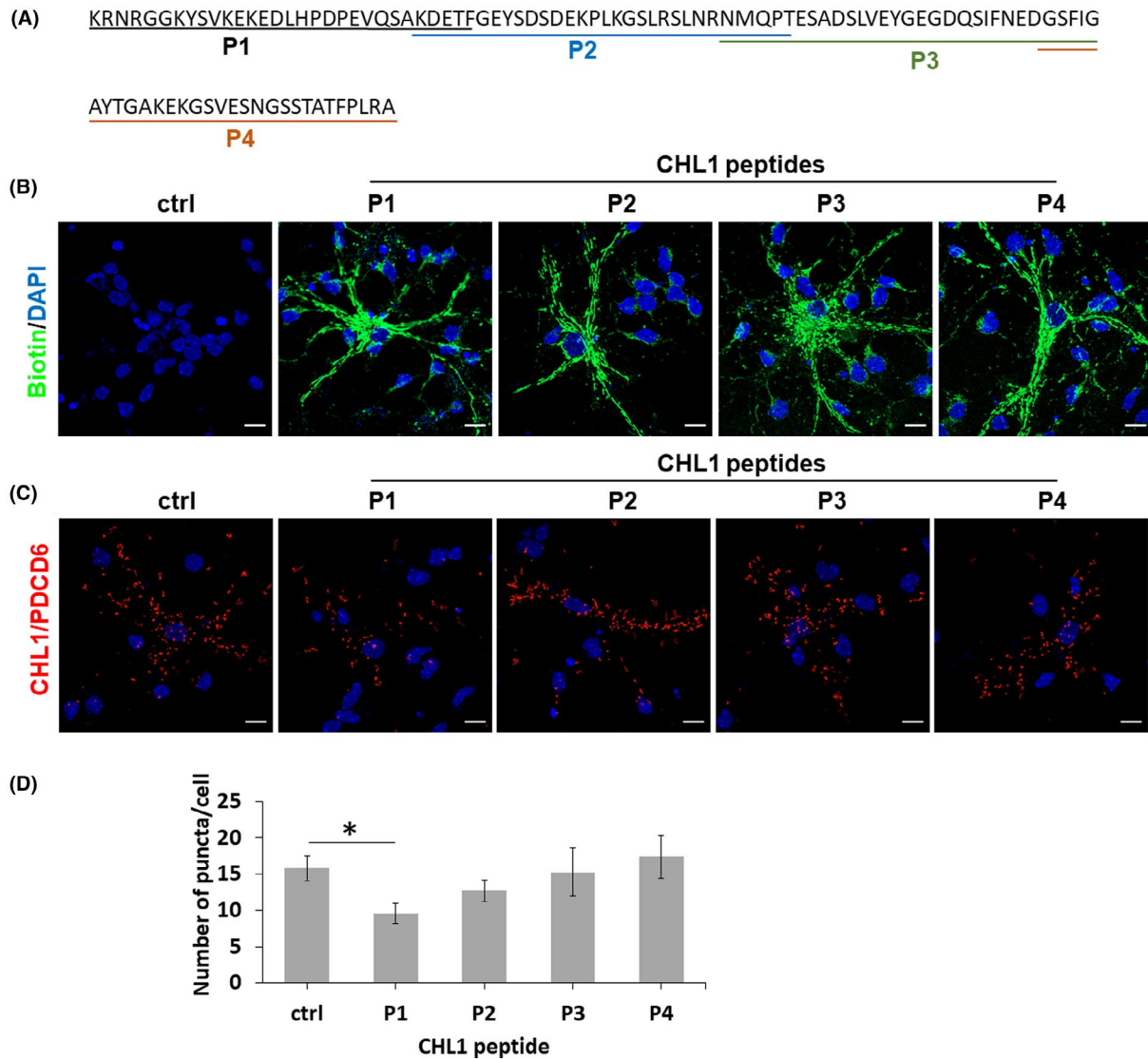


**FIGURE 6** The N-terminal 30 amino acids of the CHL1-ICD are required for the association of CHL1 with PDCD6. (A) The design of four overlapping CHL1 peptides (P1, P2, P3, and P4) is shown on the sequence of the CHL1-ICD. (B) Representative confocal images of immunofluorescence staining for biotin (green) in the cerebellar cells treated with vehicle control ( $H_2O$ , ctrl) or CHL1 peptides (P1, P2, P3, and P4). Nuclei were stained with DAPI (blue). Scale bars, 10  $\mu m$ . Of note, all peptides transfected cells with equal efficacy (one-way ANOVA with Tukey's post hoc test;  $p > 0.05$  difference between peptides P1, P2, P3, and P4). (C) Representative confocal images of immunofluorescence staining for proximity ligation assay (CHL1 + PDCD6) in the cerebellar cells treated with vehicle control ( $H_2O$ , ctrl) or CHL1 peptides P1, P2, P3, and P4. Red spots of intense fluorescent signals indicate the close proximity of CHL1 and PDCD6. Nuclei were stained with DAPI (blue). Scale bars, 10  $\mu m$ . (D) Quantification of average number of puncta in each cell of control or CHL1 peptides treated groups in (C). Data are presented as the mean  $\pm$  SEM from three independent experiments. For each analysis, 10 images from each group were analyzed (cell numbers for each group were CHL1<sup>+/+</sup>: 59 and CHL1<sup>-/-</sup>: 55). Confocal images are shown as representative results from three experiments per group. \* $p < 0.05$  with one-way ANOVA with Tukey's post hoc test

addition, none of the CHL1 peptides altered the survival of CHL1<sup>+/+</sup> and CHL1<sup>-/-</sup> neurons under basal conditions. When oxidative stress was induced by the application of hydrogen peroxide, CHL1 peptides P1–P4 did not alter the survival of both CHL1<sup>-/-</sup> and CHL1<sup>+/+</sup> neurons in the absence of CHL1Fc. Addition of CHL1Fc to the cultures reduced the death of CHL1<sup>-/-</sup> and CHL1<sup>+/+</sup> neurons when oxidative stress was induced. When cell

death was induced by hydrogen peroxide and cells were treated with CHL1Fc, adding CHL1 peptide 1 abolished the protective effect of CHL1Fc, and cell death was similar to the condition with hydrogen peroxide alone. In contrast, cell death was similar when cells were treated with hydrogen peroxide and CHL1Fc or with hydrogen peroxide, CHL1Fc and peptides P2, P3, and P4, wherein the neuroprotective effect of CHL1Fc persisted

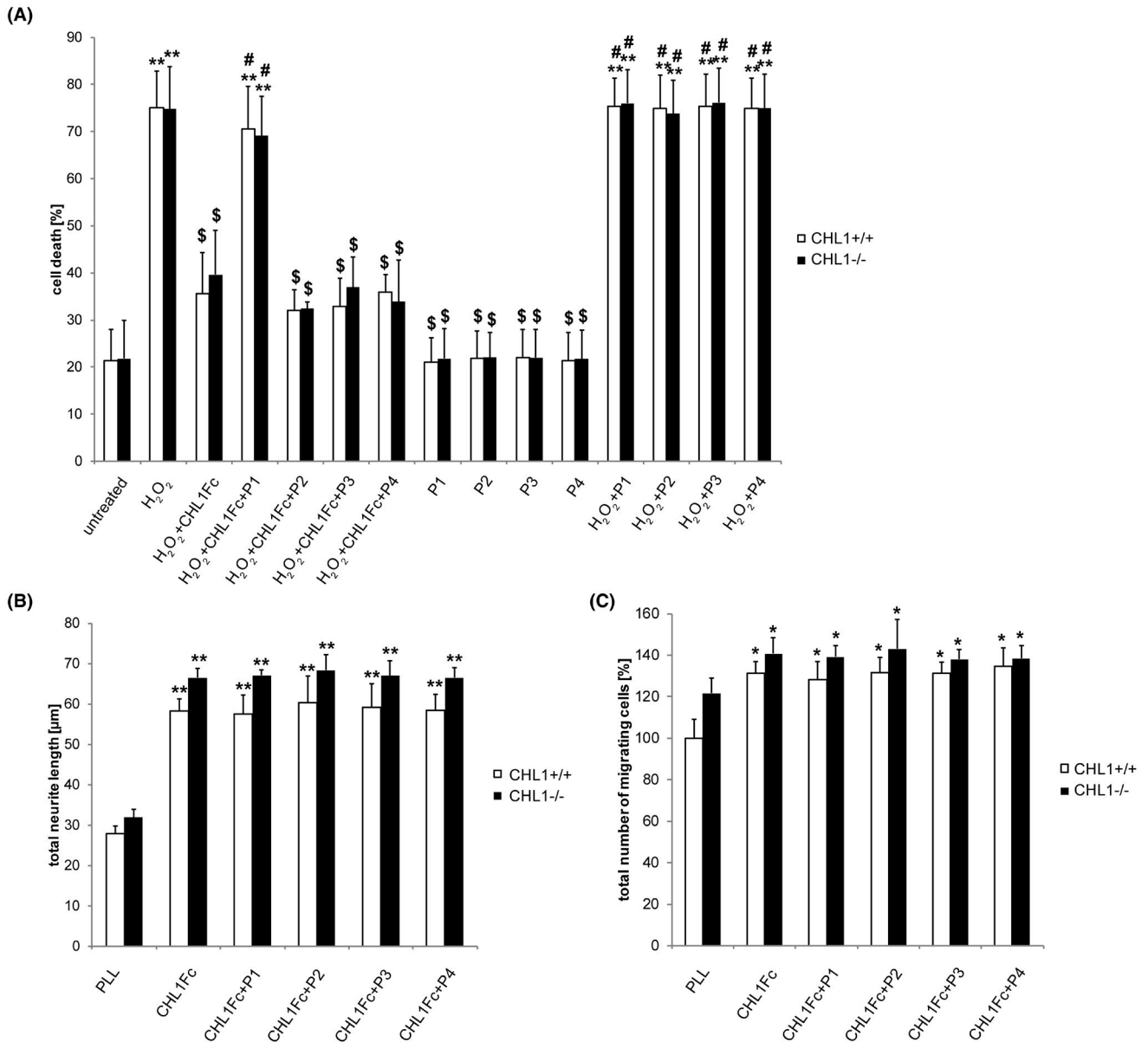


**FIGURE 7** CHL1 peptide P1 do not affect the migration and neurite outgrowth of cerebellar granule neurons, but reduces CHL1-mediated cell survival. (A) Bar diagram shows the percentage of viable cerebellar granule neurons grown on poly-L-lysine (PLL) and treated or not treated with the extracellular domain of CHL1 fused to the Fc-fragment from human IgG (CHL1Fc), CHL1 peptides P1, P2, P3, or P4, and in the presence or absence of hydrogen peroxide (H<sub>2</sub>O<sub>2</sub>) to induce cell death. Data are presented as the mean + SEM from three independent experiments (15 images captured from three wells per experiment and condition). \*\**p* < 0.01 difference relative to PLL control; \**p* < 0.05 difference relative to CHL1Fc and H<sub>2</sub>O<sub>2</sub> treated samples, \**p* < 0.05 difference relative to H<sub>2</sub>O<sub>2</sub>-treated samples, one-way ANOVA with Dunn's multiple comparison test. (B) Bar diagram shows the average neurite length of cerebellar granule neurons in the presence or absence of CHL1 peptides P1, P2, P3, or P4 and CHL1Fc. Data are presented as the mean + SEM from three independent experiments (100 neurons per experiment and condition), \*\**p* < 0.01 difference relative to PLL control, one-way ANOVA with Dunn's multiple comparison test. (C) Bar diagram shows average migration of cerebellar granule cells from explants treated with control or CHL1 peptides P1–P4 and CHL1Fc. Data are presented as the mean + SEM from four independent experiments (12 explants per experiment and condition), \**p* < 0.05 difference relative to PLL control, one-way ANOVA with Dunn's multiple comparison test

(Figure 7A). Treating the cells with CHL1 peptides P1–P4 did not change neurite length, whether the cells were maintained with or without CHL1Fc (Figure 7B; Figure S1A). Similarly, cell migration was not affected by the peptides in the absence or presence of CHL1Fc

(Figure 7C; Figure S1B). These results indicate that in unstressed cells, the peptides P1–P4 did not affect the survival, neurite outgrowth, and neuronal migration, but under oxidative stress the CHL1 peptide P1 interfered with CHL1Fc signaling and reduced the association of

CHL1 with PDCD6 or triggering of PDCD6-dependent signaling leading to reduced cell survival.

## 4 | DISCUSSION

CHL1 and PDCD6 are present in a molecular complex in early postnatal and adult mouse brains, and are co-expressed in neurons and astrocytes. The association of CHL1 and PDCD6 depends on  $\text{Ca}^{2+}$  and is mediated by the N-terminal 30 amino acids within the CHL1-ICD, comprising approximately 100 amino acids. Interestingly, a membrane-proximal motif (RGGKYSV) within the N-terminal 30 amino acids of CHL1-ICD that mediates the interaction with PDCD6 is also required for recruiting ezrin, a member of the ezrin–radixin–moesin (ERM) family of filamentous actin-binding proteins.<sup>55</sup> The RGGKYSV motif in CHL1 is important for semaphorin3A-induced growth cone collapse as well as CHL1-dependent neurite outgrowth and branching in cortical embryonic neurons.<sup>55</sup> In addition, stimulation of haptotactic cell migration and cellular adhesion to fibronectin by CHL1 depends on this CHL1/ERM recruitment motif.<sup>55</sup> The HPD tripeptide that mediates the interaction between CHL1 and Hsc70 is also present in the first N-terminal 30 amino acids of CHL1-ICD.<sup>34</sup>

The CHL1 peptide P3, which includes the ankyrin recruitment region FIG[AQ]Y, does not interfere with the CHL1/PDCD6 association, suggesting that binding to ankyrin on the cytoskeleton is not important for this association and for down-stream signaling effects. For other CHL1-ICD interaction partners, such as serotonin receptor 2c, the site of interaction has not been specified<sup>32</sup> (Figure S2). Interaction with this receptor is noteworthy because mutations and polymorphisms in human CHL1, named CALL, and gene duplications and deletions of the chromosomal region 3p26 that contains also CHL1, are linked to autism spectrum disorder, schizophrenia, and 3p syndrome.<sup>25,35,56–58</sup> Deletions within the 3p26 chromosomal region are often caused by de novo mutations within this region, but no disease-causing mutations were reported for CHL1-ICD, making it difficult to judge if the loss of the extracellular domain or the ICD of CHL1 underlies the functional defects observed.

CHL1 peptide P1 derived from the N-terminus of the CHL1-ICD reduced CHL1Fc-mediated neuronal survival in CHL1<sup>-/-</sup> and CHL1<sup>+/+</sup> cells, whereas peptides derived from the intermediate and C-terminal part of the CHL1-ICD did not affect the neuronal survival. Interestingly, the CHL1 peptide P1 reduces the cell survival of CHL1<sup>-/-</sup> and CHL1<sup>+/+</sup> cells, in the presence of the stimulating agent CHL1Fc, suggesting that CHL1 peptide 1 not only blocks triggering of heterophilic CHL1 interactions but also

interaction of CHL1 with PDCD6. Furthermore, CHL1 peptide P1 may interfere with interactions of CHL1 with the binding partners ezrin, patched-1, or Hsc70 to affect cell survival.

The observation that CHL1-ICD peptides do not affect neurite outgrowth and migration of cerebellar neurons suggests that CHL1 association with PDCD6 is mainly important for cell survival (Figure S3). This agrees with previous reports on CHL1 or PDCD6 regarding cell survival.<sup>12,23,48,59–61</sup> PDCD6 expression in CHL1-deficient mouse brains is normal and similar during development and in adulthood, suggesting that PDCD6 engages with binding partners other than CHL1 that could contribute to maintaining its normal levels. Interestingly, CHL1 peptide P1, which contains the RGGKYSV motif involved in cortical neuron outgrowth,<sup>55</sup> did not affect the cerebellar neuronal outgrowth in our study. These results suggest that the ERM motif within CHL1-ICD is not important for neurite outgrowth of cerebellar neurons nor is it required for early postnatal development.

Other studies showed that CHL1 triggers patched-1- and smoothed-dependent signal transduction pathways to promote neuronal survival in murine cerebellum and that CHL1-deficient mice show abnormal death of cerebellar granule cells during the second postnatal week.<sup>12</sup> CHL1-deficient mice show increased numbers of caspase-3- and NeuN-positive neurons in the internal granule layer at postnatal days 10 and 14 when compared to their wild-type littermates, suggesting that this cell death may be caspase-3-dependent.<sup>12</sup> In addition, juvenile CHL1-deficient mice show abnormally high numbers of parvalbumin-expressing hippocampal interneurons, but a loss of these cells is observed in CHL1-deficient adult mice.<sup>23</sup> Whether or not these cells are eliminated via caspase-3-dependent mechanisms was not determined. Cell death via a caspase-3-dependent pathway occurs after co-transfection of PDCD6 and death-associated protein kinase 1 cDNA into a tumor cell line, while transfection of PDCD6 alone did not change caspase-3 activity.<sup>40</sup> Human ovarian carcinoma cells over-expressing PDCD6 showed activation of caspase-3, -8, and -9 as well as inhibited cell growth, and caspase-3 and -9 inhibitors protected cells from PDCD6-induced apoptosis.<sup>59</sup> Induction of tumor cell death and knock-down of PDCD6 led to suppression of caspase-3 activation.<sup>60</sup> We here show that levels of PDCD6 are unaltered in CHL1-deficient brains and thus cannot account for the different levels of cell death seen in the cerebellum in the second postnatal week. Yet, interaction or association of CHL1 and PDCD6 could influence caspase-3-dependent neuronal death during this time period. Since PDCD6 does not only act upstream, but also downstream of the caspase signaling cascade,<sup>61</sup> CHL1 may also influence PDCD6 activity via regulation

of caspase activities. Interestingly, PDCD6-deficient mice develop normally,<sup>39</sup> whereas CHL1-deficient mice show a significant loss of Purkinje and granule cells in the adult cerebellum,<sup>54</sup> indicating different functions for CHL1 and PDCD6 during brain development.

In addition to its functions in the nervous system, CHL1 is involved in tumor growth. It is a tumor suppressor in many tumors, such as neuroblastoma, nasopharyngeal carcinoma, esophageal squamous cell carcinoma, and non-small cell lung cancer.<sup>62–65</sup> Reduced tissue expression and enhanced serum levels of CHL1 in gastrointestinal stroma tumors correlate with advances of tumor stages and shorter recurrence-free survival.<sup>66</sup> CHL1 also promotes cell proliferation, and metastasis of human glioma cells both in vitro and in vivo, and CHL1 expression is upregulated in glioblastoma cells.<sup>67</sup> Interestingly, in xenograft tumors in nude mice, administration of siRNA targeting CHL1 not only downregulates CHL1 expression in vivo, but also upregulates activated caspase-3 levels.<sup>67</sup> Caspase-3 upregulation in glioblastoma after knock-down of CHL1 is consistent with enhanced caspase-3 activity found in cerebella of CHL1-deficient mice, suggesting that CHL1 influences caspase-3 activation. Like CHL1, PDCD6 expression is upregulated in several tumors and high levels of PDCD6 are a poor prognostic factor in lung adenocarcinoma, while low levels are correlated with poor survival of gastric cancer patients.<sup>68,69</sup> PDCD6 also stimulates cell migration and invasion of metastatic ovarian cancer cells.<sup>70</sup> These studies indicate that upregulation of CHL1 and PDCD6 in tumors can be a good or bad prognostic sign depending on the tumor type and that both proteins may suppress or enhance tumor growth. Nevertheless, both proteins influence cell migration and survival in the tumor context where they might cooperate.

Both CHL1 and PDCD6 affect vesicle functions, such as trafficking or uncoating: CHL1 deficiency reduces targeting of Hsc70 to the synaptic plasma membrane and disrupts the CHL1/Hsc70 complex, resulting in accumulation of abnormally high levels of clathrin-coated vesicles with a reduced ability to release clathrin.<sup>34</sup> PDCD6 has not yet been shown to influence synaptic vesicle transport but is involved in non-synaptic vesicle transport. These functions are linked to the Ca<sup>2+</sup>-dependent interaction of PDCD6 with various proteins that function in the endosomal sorting complex required for the transport (ESCRT) system and regulation of endoplasmic reticulum (ER)-to-Golgi vesicular transport.<sup>71</sup> Via interaction with Sec31A, a component of the coat protein complex II, PDCD6 regulates vesicle trafficking and cargo packaging.<sup>72</sup> In addition, several PDCD6 targets are physically and functionally associated with the plasma or organelle membranes (reviewed in Ref.<sup>71</sup>), indicating a role for PDCD6 in membrane-linked processes. Alix, also called AIP1, was

the first PDCD6-binding protein identified,<sup>73,74</sup> and it is associated with components of the ESCRT system, which is important in a plethora of cellular processes associated with membrane remodeling, including endosome formation, fusion of autophagosomes and amphisomes with lysosomes, as well as plasma and nuclear envelope membrane repair (reviewed in Refs.<sup>75,76</sup>). CHL1 together with PDCD6 and Alix could also play a role in membrane remodeling and repair. This would be an interesting topic for future investigations.

## ACKNOWLEDGMENTS

The authors are grateful to Jennifer Nguyen and Yuliya Hapiak for genotyping, Drs Hyeon-Yeol Cho and KiBum Lee for generous advice on CHL1 peptide transfection, and Dr. Fritz Buck and Sönke Harder for mass spectrometry.

## CONFLICT OF INTEREST

None declared.

## AUTHOR CONTRIBUTIONS

MS, GL, RK, and TT conceived the study and designed experiments. GL, RK, HBH, TT, SA, JS, NS, and NA performed the experiments. WY contributed with discussions. HBH, GL, and MS wrote the paper.

## ORCID

Thomas Theis  <https://orcid.org/0000-0001-5555-8501>

Ralf Kleene  <https://orcid.org/0000-0002-5935-5266>

## REFERENCES

1. Maness PF, Schachner M. Neural recognition molecules of the immunoglobulin superfamily: signaling transducers of axon guidance and neuronal migration. *Nat Neurosci.* 2007;10:19-26.
2. Panicker AK, Buhusi M, Thelen K, Maness PF. Cellular signalling mechanisms of neural cell adhesion molecules. *Front Biosci.* 2003;8:d900-911.
3. Walsh FS, Doherty P. Neural cell adhesion molecules of the immunoglobulin superfamily: role in axon growth and guidance. *Annu Rev Cell Dev Biol.* 1997;13:425-456.
4. Sytnyk V, Leshchyn'ska I, Schachner M. Neural cell adhesion molecules of the immunoglobulin superfamily regulate synapse formation, maintenance and function. *Trends Neurosci.* 2017;40:295-308.
5. Hillenbrand R, Molthagen M, Montag D, Schachner M. The close homologue of the neural adhesion molecule L1 (CHL1): patterns of expression and promotion of neurite outgrowth by heterophilic interactions. *Eur J Neurosci.* 1999;11:813-826.
6. Holm J, Hillenbrand R, Steuber V, et al. Structural features of a close homologue of L1 (CHL1) in the mouse: a new member of the L1 family of neural recognition molecules. *Eur J Neurosci.* 1996;8:1613-1629.
7. Buhusi M, Midkiff BR, Gates AM, Richter M, Schachner M, Maness PF. Close homolog of L1 is an enhancer of integrin-mediated cell migration. *J Biol Chem.* 2003;278:25024-25031.

8. Chaisuksunt V, Campbell G, Zhang Y, Schachner M, Lieberman AR, Anderson PN. The cell recognition molecule CHL1 is strongly upregulated by injured and regenerating thalamic neurons. *J Comp Neurol.* 2000;425:382-392.
9. Demyanenko GP, Schachner M, Anton E, et al. Close homolog of L1 modulates area-specific neuronal positioning and dendrite orientation in the cerebral cortex. *Neuron.* 2004;44:423-437.
10. Dong L, Chen S, Richter M, Schachner M. Single-chain variable fragment antibodies against the neural adhesion molecule CHL1 (close homolog of L1) enhance neurite outgrowth. *J Neurosci Res.* 2002;69:437-447.
11. Katic J, Loers G, Kleene R, et al. Interaction of the cell adhesion molecule CHL1 with vitronectin, integrins, and the plasminogen activator inhibitor-2 promotes CHL1-induced neurite outgrowth and neuronal migration. *J Neurosci.* 2014;34:14606-14623.
12. Katic J, Loers G, Tosic J, Schachner M, Kleene R. The cell adhesion molecule CHL1 interacts with patched-1 to regulate apoptosis during postnatal cerebellar development. *J Cell Sci.* 2017;130:2606-2619.
13. Liu Q, Dwyer ND, O'Leary DDM. Differential expression of COUP-TFI, CHL1, and two novel genes in developing neocortex identified by differential display PCR. *J Neurosci.* 2000;20:7682-7690.
14. Ye H, Tan YLJ, Ponniah S, et al. Neural recognition molecules CHL1 and NB-3 regulate apical dendrite orientation in the neocortex via PTPalpha. *EMBO J.* 2008;27:188-200.
15. Ango F, Wu C, Van der Want JJ, Wu P, Schachner M, Huang ZJ. Bergmann glia and the recognition molecule CHL1 organize GABAergic axons and direct innervation of Purkinje cell dendrites. *PLoS Biol.* 2008;6:e103.
16. Demyanenko GP, Siesser PF, Wright AG, et al. L1 and CHL1 cooperate in thalamocortical axon targeting. *Cereb Cortex.* 2011;21:401-412.
17. Irintchev A, Koch M, Needham LK, Maness P, Schachner M. Impairment of sensorimotor gating in mice deficient in the cell adhesion molecule L1 or its close homologue, CHL1. *Brain Res.* 2004;1029:131-134.
18. Kolata S, Wu J, Light K, Schachner M, Matzel LD. Impaired working memory duration but normal learning abilities found in mice that are conditionally deficient in the close homolog of L1. *J Neurosci.* 2008;28:13505-13510.
19. Morellini F, Lepsveridze E, Kähler B, Dityatev A, Schachner M. Reduced reactivity to novelty, impaired social behavior, and enhanced basal synaptic excitatory activity in perforant path projections to the dentate gyrus in young adult mice deficient in the neural cell adhesion molecule CHL1. *Mol Cell Neurosci.* 2007;34:121-136.
20. Montag-Sallaz M, Schachner M, Montag D. Misguided axonal projections, neural cell adhesion molecule 180 mRNA upregulation, and altered behavior in mice deficient for the close homolog of L1. *Mol Cell Biol.* 2002;22:7967-7981.
21. Nikonenko AG, Sun M, Lepsveridze E, et al. Enhanced perisomatic inhibition and impaired long-term potentiation in the CA1 region of juvenile CHL1-deficient mice. *Eur J Neurosci.* 2006;23:1839-1852.
22. Pratte M, Jamon M. Impairment of novelty detection in mice targeted for the Chl1 gene. *Physiol Behav.* 2009;97:394-400.
23. Schmalbach B, Lepsveridze E, Djogo N, et al. Age-dependent loss of parvalbumin-expressing hippocampal interneurons in mice deficient in CHL1, a mental retardation and schizophrenia susceptibility gene. *J Neurochem.* 2015;135:830-844.
24. Angeloni D, Lindor NM, Pack S, Latif F, Wei MH, Lerman MI. CALL gene is haploinsufficient in a 3p-syndrome patient. *Am J Med Genet.* 1999;86:482-485.
25. Chen QY, Chen Q, Feng GY, et al. Case-control association study of the close homologue of L1 (CHL1) gene and schizophrenia in the Chinese population. *Schizophr Res.* 2005;73:269-274.
26. Cuoco C, Ronchetto P, Gimelli S, et al. Microarray based analysis of an inherited terminal 3p26.3 deletion, containing only the CHL1 gene, from a normal father to his two affected children. *Orphanet J Rare Dis.* 2011;6:12.
27. Frints SGM, Marynen P, Hartmann D, et al. CALL interrupted in a patient with non-specific mental retardation: gene dosage-dependent alteration of murine brain development and behavior. *Hum Mol Genet.* 2003;12:1463-1474.
28. Sakurai K, Migita O, Toru M, Arinami T. An association between a missense polymorphism in the close homologue of L1 (CHL1, CALL) gene and schizophrenia. *Mol Psychiatry.* 2002;7:412-415.
29. Salyakina D, Cukier HN, Lee JM, et al. Copy number variants in extended autism spectrum disorder families reveal candidates potentially involved in autism risk. *PLoS One.* 2011;6:e26049.
30. Shoukier M, Fuchs S, Schwaibold E, et al. Microduplication of 3p26.3 in nonsyndromic intellectual disability indicates an important role of CHL1 for normal cognitive function. *Neuropediatrics.* 2013;44:268-271.
31. Jakovcevski I, Wu J, Karl N, et al. Glial scar expression of CHL1, the close homolog of the adhesion molecule L1, limits recovery after spinal cord injury. *J Neurosci.* 2007;27:7222-7233.
32. Kleene R, Chaudhary H, Karl N, et al. Interaction between CHL1 and serotonin receptor 2c regulates signal transduction and behavior in mice. *J Cell Sci.* 2015;128:4642-4652.
33. Wright AG, Demyanenko GP, Powell A, et al. Close homolog of L1 and neuropilin 1 mediate guidance of thalamocortical axons at the ventral telencephalon. *J Neurosci.* 2007;27:13667-13679.
34. Leshchyn'ska I, Sytnyk V, Richter M, Andreyeva A, Puchkov D, Schachner M. The adhesion molecule CHL1 regulates uncoating of clathrin-coated synaptic vesicles. *Neuron.* 2006;52:1011-1025.
35. Andreyeva A, Leshchyn'ska I, Knepper M, et al. CHL1 is a selective organizer of the presynaptic machinery chaperoning the SNARE complex. *PLoS One.* 2010;5:e12018.
36. Tian N, Leshchyn'ska I, Welch JH, et al. Lipid raft-dependent endocytosis of close homolog of adhesion molecule L1 (CHL1) promotes neuritogenesis. *J Biol Chem.* 2012;287:44447-44463.
37. Maki M, Yamaguchi K, Kitaura Y, Satoh H, Hitomi K. Calcium-induced exposure of a hydrophobic surface of mouse ALG-2, which is a member of the penta-EF-hand protein family. *J Biochem.* 1998;124:1170-1177.
38. Vito P, Lacaná E, D'Adamo L. Interfering with apoptosis: Ca<sup>2+</sup>-binding protein ALG-2 and Alzheimer's disease gene ALG-3. *Science.* 1996;271:521-525.
39. Jang IK, Hu R, Lacana E, D'Adamo L, Gu H. Apoptosis-linked gene 2-deficient mice exhibit normal T-cell development and function. *Mol Cell Biol.* 2002;22:4094-4100.
40. Lee JH, Rho SB, Chun T. Programmed Cell Death 6 (PDCD6) protein interacts with death-associated protein kinase 1 (DAPK1): additive effect on apoptosis via caspase-3 dependent pathway. *Biotechnol Lett.* 2005;27:1011-1015.

41. Mahul-Mellier AL, Hemming FJ, Blot B, Fraboulet S, Sadoul R. Alix, making a link between apoptosis-linked gene-2, the endosomal sorting complexes required for transport, and neuronal death in vivo. *J Neurosci*. 2006;26:542-549.
42. Rao RV, Poksay KS, Castro-Obregon S, et al. Molecular components of a cell death pathway activated by endoplasmic reticulum stress. *J Biol Chem*. 2004;279:177-187.
43. Katoh K, Suzuki H, Terasawa Y, et al. The penta-EF-hand protein ALG-2 interacts directly with the ESCRT-I component TSG101, and Ca<sup>2+</sup>-dependently co-localizes to aberrant endosomes with dominant-negative AAA ATPase SKD1/Vps4B. *Biochem J*. 2005;391:677-685.
44. McGourty CA, Akopian D, Walsh C, et al. Regulation of the CUL3 ubiquitin ligase by a calcium-dependent co-adaptor. *Cell*. 2016;167:525-538.e514.
45. Shibata H, Suzuki H, Kakiuchi T, et al. Identification of Alix-type and non-Alix-type ALG-2-binding sites in human phospholipid scramblase 3 differential binding to an alternatively spliced isoform and amino acid-substituted mutants. *J Biol Chem*. 2008;283:9623-9632.
46. Vergarajauregui S, Martina JA, Puertollano R. Identification of the penta-EF-hand protein ALG-2 as a Ca<sup>2+</sup>-dependent interactor of mucolipin-1. *J Biol Chem*. 2009;284:36357-36366.
47. Cassens C, Kleene R, Xiao MF, et al. Binding of the receptor tyrosine kinase TrkB to the neural cell adhesion molecule (NCAM) regulates phosphorylation of NCAM and NCAM-dependent neurite outgrowth. *J Biol Chem*. 2010;285:28959-28967.
48. Chen S, Mantei N, Dong L, Schachner M. Prevention of neuronal cell death by neural adhesion molecules L1 and CHL1. *J Neurobiol*. 1999;38:428-439.
49. Wang S, Cesca F, Loers G, et al. Synapsin I is an oligomannose-carrying glycoprotein, acts as an oligomannose-binding lectin, and promotes neurite outgrowth and neuronal survival when released via glia-derived exosomes. *J Neurosci*. 2011;31:7275-7290.
50. Makhina T, Loers G, Schulze C, Ueberle B, Schachner M, Kleene R. Extracellular GAPDH binds to L1 and enhances neurite outgrowth. *Mol Cell Neurosci*. 2009;41:206-218.
51. Xiao MF, Xu JC, Tereshchenko Y, Novak D, Schachner M, Kleene R. Neural cell adhesion molecule modulates dopaminergic signaling and behavior by regulating dopamine D2 receptor internalization. *J Neurosci*. 2009;29:14752-14763.
52. Kleene R, Loers G, Langer J, Frobert Y, Buck F, Schachner M. Prion protein regulates glutamate-dependent lactate transport of astrocytes. *J Neurosci*. 2007;27:12331-12340.
53. Loers G, Chen S, Grumet M, Schachner M. Signal transduction pathways implicated in neural recognition molecule L1 triggered neuroprotection and neuritogenesis. *J Neurochem*. 2005;92:1463-1476.
54. Jakovcevski I, Siering J, Hargus G, et al. Close homologue of adhesion molecule L1 promotes survival of Purkinje and granule cells and granule cell migration during murine cerebellar development. *J Comp Neurol*. 2009;513:496-510.
55. Schlatter MC, Buhusi M, Wright AG, Maness PF. CHL1 promotes Sema3A-induced growth cone collapse and neurite elaboration through a motif required for recruitment of ERM proteins to the plasma membrane. *J Neurochem*. 2008;104:731-744.
56. Firth HV, Richards SM, Bevan AP, et al. DECIPHER: database of chromosomal imbalance and phenotype in humans using ensembl resources. *Am J Hum Genet*. 2009;84:524-533.
57. Fernandez TV, Garcia-Gonzalez IJ, Mason CE, et al. Molecular characterization of a patient with 3p deletion syndrome and a review of the literature. *Am J Med Genet A*. 2008;146A:2746-2752.
58. Li C, Liu C, Zhou B, Hu C, Xu X. Novel microduplication of CHL1 gene in a patient with autism spectrum disorder: a case report and a brief literature review. *Mol Cytogenet*. 2016;9:51.
59. Park SH, Lee JH, Le GB, et al. PDCD6 additively cooperates with anti-cancer drugs through activation of NF-kappaB pathways. *Cell Signal*. 2012;24:726-733.
60. Suzuki K, Dashzeveg N, Lu ZG, Taira N, Miki Y, Yoshida K. Programmed cell death 6, a novel p53-responsive gene, targets to the nucleus in the apoptotic response to DNA damage. *Cancer Sci*. 2012;103:1788-1794.
61. Lacana E, Ganjei JK, Vito P, D'Adamio L. Dissociation of apoptosis and activation of IL-1beta-converting enzyme/Ced-3 proteases by ALG-2 and the truncated Alzheimer's gene ALG-3. *J Immunol*. 1997;158:5129-5135.
62. Ognibene M, Pagnan G, Marimpietri D, et al. CHL1 gene acts as a tumor suppressor in human neuroblastoma. *Oncotarget*. 2018;9:25903-25921.
63. Chen J, Jiang C, Fu L, et al. CHL1 suppresses tumor growth and metastasis in nasopharyngeal carcinoma by repressing PI3K/AKT signaling pathway via interaction with Integrin beta1 and Merlin. *Int J Biol Sci*. 2019;15:1802-1815.
64. Tang H, Jiang L, Zhu C, et al. Loss of cell adhesion molecule L1 like promotes tumor growth and metastasis in esophageal squamous cell carcinoma. *Oncogene*. 2019;38:3119-3133.
65. Hötzel J, Melling N, Muller J, et al. Protein expression of close homologue of L1 (CHL1) is a marker for overall survival in non-small cell lung cancer (NSCLC). *J Cancer Res Clin Oncol*. 2019;145:2285-2292.
66. Karstens KF, Bellon E, Polonski A, et al. Expression and serum levels of the neural cell adhesion molecule L1-like protein (CHL1) in gastrointestinal stroma tumors (GIST) and its prognostic power. *Oncotarget*. 2020;11:1131-1140.
67. Yang Z, Xie Q, Hu CL, et al. CHL1 is expressed and functions as a malignancy promoter in glioma cells. *Front Mol Neurosci*. 2017;10:324.
68. la Cour JM, Mollerup J, Winding P, Tarabykina S, Sehested M, Berchtold MW. Up-regulation of ALG-2 in hepatomas and lung cancer tissue. *Am J Pathol*. 2003;163:81-89.
69. Yamada Y, Arai T, Gotoda T, et al. Identification of prognostic biomarkers in gastric cancer using endoscopic biopsy samples. *Cancer Sci*. 2008;99:2193-2199.
70. Su D, Xu H, Feng J, et al. PDCD6 is an independent predictor of progression free survival in epithelial ovarian cancer. *J Transl Med*. 2012;10:31.
71. Maki M, Takahara T, Shibata H. Multifaceted roles of ALG-2 in Ca<sup>2+</sup>-regulated membrane trafficking. *Int J Mol Sci*. 2016;17:1401.
72. la Cour JM, Schindler AJ, Berchtold MW, Schekman R. ALG-2 attenuates COPII budding in vitro and stabilizes the Sec23/Sec31A complex. *PLoS One*. 2013;8:e75309.
73. Vito P, Pellegrini L, Guiet C, D'Adamio L. Cloning of AIP1, a novel protein that associates with the apoptosis-linked gene ALG-2 in a Ca<sup>2+</sup>-dependent reaction. *J Biol Chem*. 1999;274:1533-1540.
74. Missotten M, Nichols A, Rieger K, Sadoul R. Alix, a novel mouse protein undergoing calcium-dependent interaction with the apoptosis-linked-gene 2 (ALG-2) protein. *Cell Death Differ*. 1999;6:124-129.

75. Hurley JH. ESCRTs are everywhere. *EMBO J*. 2015;34:2398-2407.
76. Christ L, Raiborg C, Wenzel EM, Campsteijn C, Stenmark H. Cellular functions and molecular mechanisms of the ESCRT membrane-scission machinery. *Trends Biochem Sci*. 2017;42:42-56.

### SUPPORTING INFORMATION

Additional supporting information may be found online in the Supporting Information section.

**How to cite this article:** Loers G, Theis T, Baixia Hao H, et al. Interplay in neural functions of cell adhesion molecule close homolog of L1 (CHL1) and Programmed Cell Death 6 (PDCD6). *FASEB BioAdvances*. 2022;4:43–59. <https://doi.org/10.1096/fba.2021-00027>